Geophysical Research Letter

Supporting Information for

Changes in the response of the Northern Hemisphere carbon uptake to temperature over the last three decades

Yi Yin[1,2], Philippe Ciais[2], Frederic Chevallier[2], Wei Li[2], Ana Bastos[2], Shilong Piao[3,4], Tao Wang[4], Hongyan Liu[3]

[1]California Institute of Technology, Pasadena, CA, USA
[2]Laboratoire des Sciences du Climat et de l'Environnement, CEA-CNRS-UVSQ, UMR8212, Gif-sur-Yvette, France
[3]Department of Ecology, College of Urban and Environmental Sciences, Peking University, China
[4]Key Laboratory of Alpine Ecology and Biodiversity, Institute of Tibetan Plateau Research, Chinese Academy of Sciences, Beijing, China

Corresponding author: Yi Yin (yiyin@caltech.edu)

Contents of this file

Figure S1. Spatial distribution of surface CO_2 stations norther of 30°N. The colors show the strongest correlations found using 10-yr moving window over the period of the pre-2000 period and the post-2000 period. Squares represent significant correlations at the 90% confidence level.

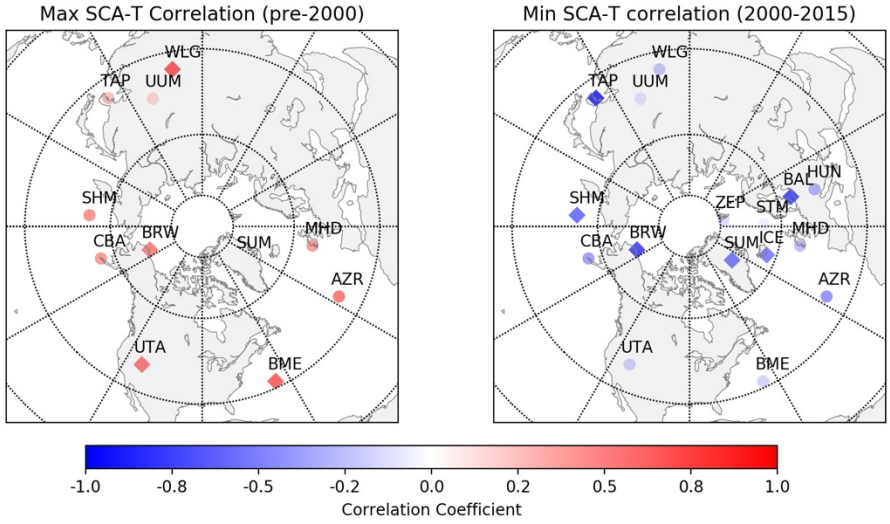

Figure S2. Temporal changes in the trends of (a) SCA at Barrow, (b) the NH air temperature in the 30-80°N zone, (c) minimum CO_2 dates in the CO_2 draw-down troughs, and (d) maximum CO_2 dates in the CO_2 peaks. Trends were analyzed using a certain moving window; the color codes represent different window lengths (10-yr, 15-yr, or 20-yr) and each data point is drawn at the middle of the analyzing window; the shaded areas show the standard deviations of the trends estimated using a bootstrap method; the colored stars mark significant correlations at the 90% confidence level.

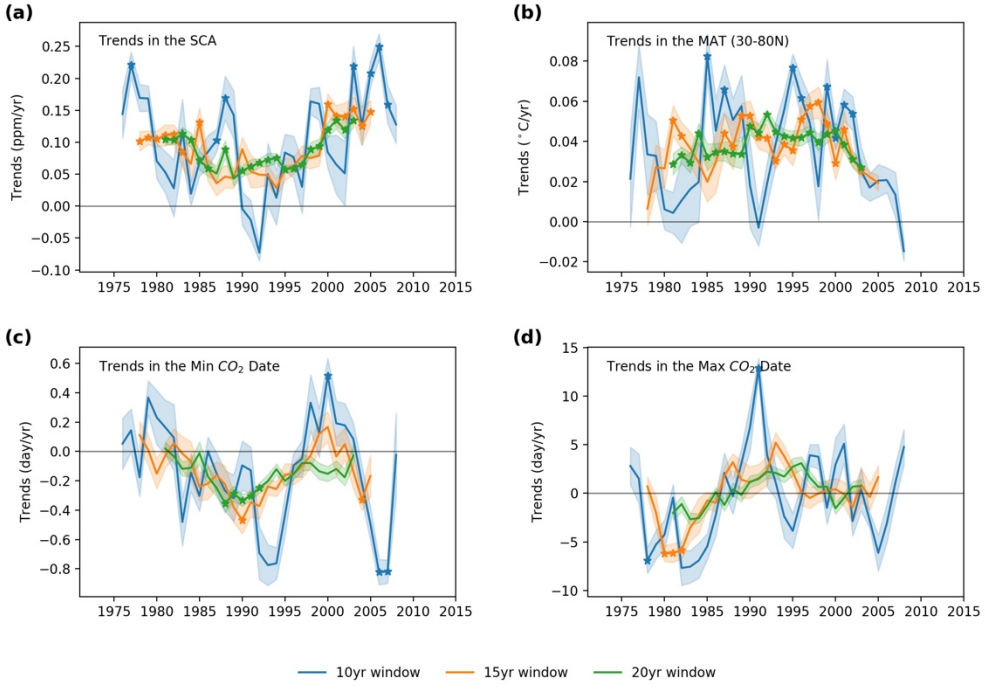

Figure S3. Inverted NBP fluxes from the three atmospheric inversions in the four seasons. Note that for the JENA_s04 inversion, results outside its validity period 2004–2015 that does not have consistent network constraint, are shown in dashed lines.

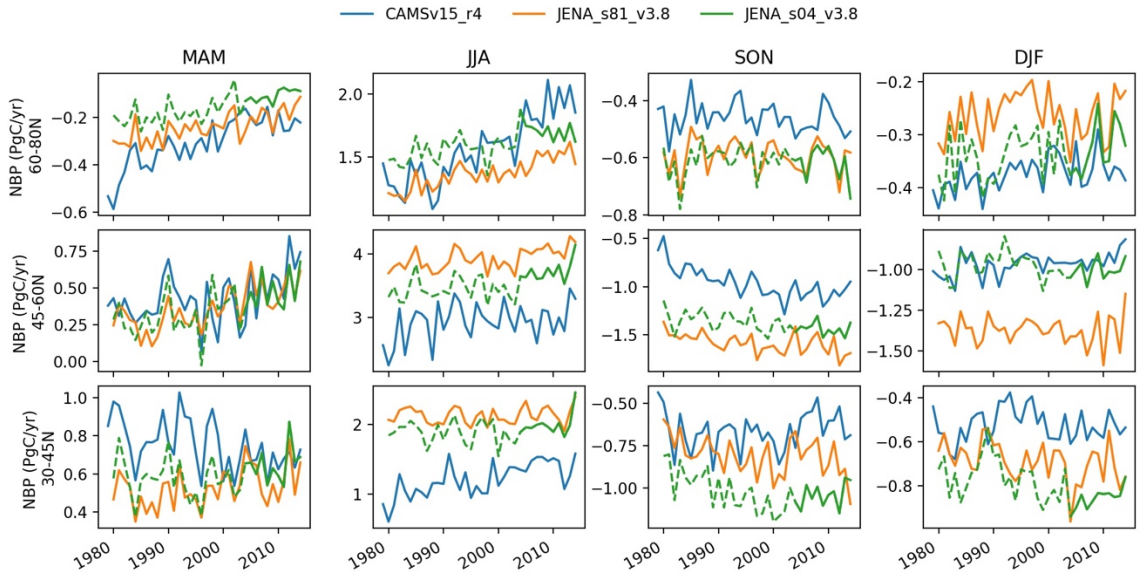

Figure S4. Spatial distribution of the correlations between MODIS NDVI anomalies and T anomalies in the four seasons for the period of 2000-2014.

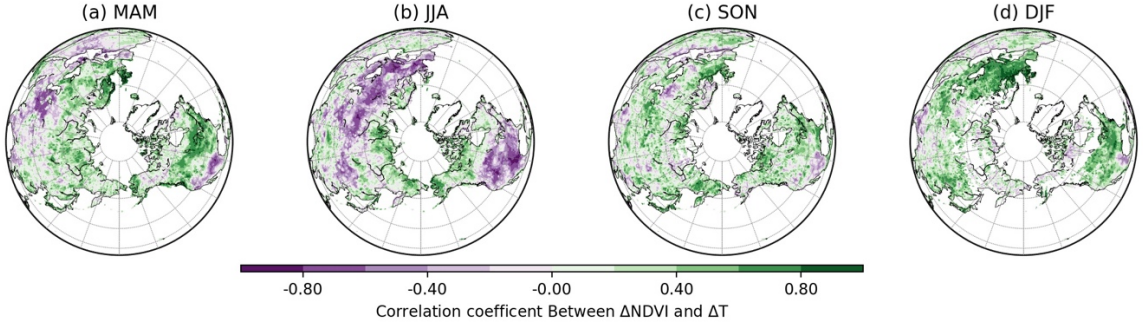

Figure S5. Correlations between climate indexes in the period of 1973-1999 (left) and 2000-2014 (right). Each small cubic (4×4) outlined by black squares represents the correlation matrix between certain variables across the four seasons (in the order from spring to winter). The diagonal term represent correlations in the same season and the off diagonal term represent correlations in different seasons. The subscript *H* represents high-latitudes 60-80°N, and *M* represents mid-latitudes 30-60°N. T and P represent temperature and precipitation from the CRU TS 4.1. SM represents soil moisture from three data sets, the ESA CCI[1], the NOAA CPC[2], and the GLEAM[3] described in the annotation below.

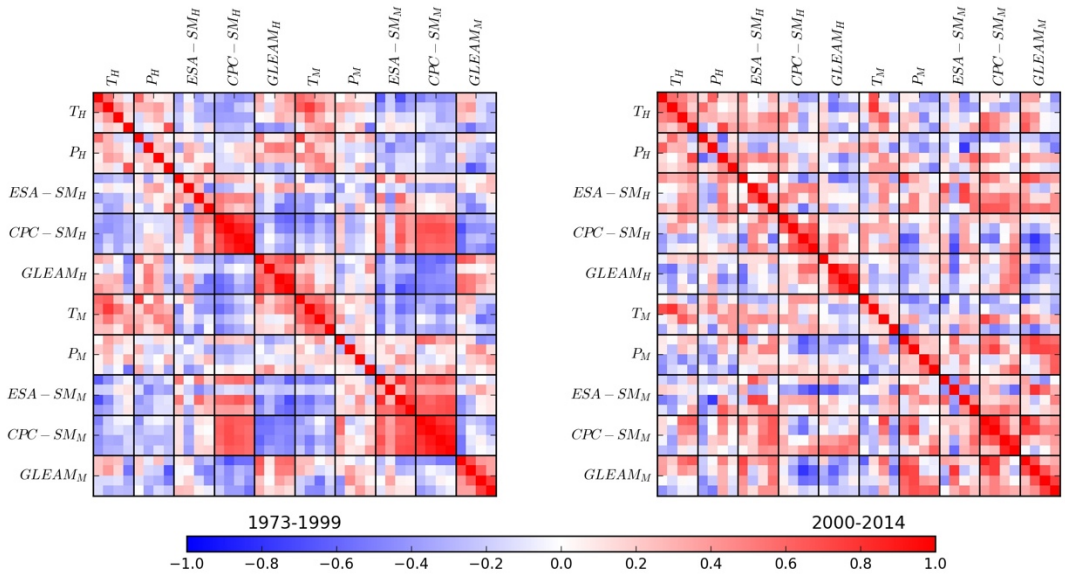

1. The global ESA CCI soil moisture product derived from satellite observations of top-soil moisture (v2.2, available at: http://www.esa-soilmoisture-cci.org/, [*Dorigo et al.*, 2015]). It provides daily top-soil (10 cm) moisture retrieved from microwave sensors with a spatial resolution of 25 km. In this work, we used the combined active and passive product that covers the period from 1979 to 2014. In this product, winter measurements are not available in the high latitudes when soils are frozen.

2. NOAA Climate Prediction Center (CPC) model estimated soil moisture from a one-layer "bucket" water balance model (V2, http://www.esrl.noaa.gov/psd/data/gridded/data.cpcsoil.html, [*Fan and van den Dool*, 2004]. It provides monthly soil moisture at a spatial resolution of 0.5 from 1948 to 2016.

3. The Global Land Evaporation Amsterdam Model (GLEAM) soil moisture derived from data driven evapotranspiration model assimilated against microwave remote sensing data (v3.0a, available at: http://www.gleam.eu/, [*Martens et al.*, 2016]). It estimates daily terrestrial evapotranspiration rate (and of its components including transpiration, bare-soil evaporation, open-water evaporation, interception loss and sublimation), as well as surface and root-zone soil moisture, with a spatial resolution of 0.25°. We used the v3.0a data, covering the period from 1980 to 2014.

Figure S6. Spatial distribution of the temporal trends in the correlation coefficients between ΔNBP and ΔT using a 10-yr moving window for the four seasons. The results are based on the JENA_s81 inversion for the period 1981-2015; the green stars show the spatial distribution of the stations being assimilated in this inversion.

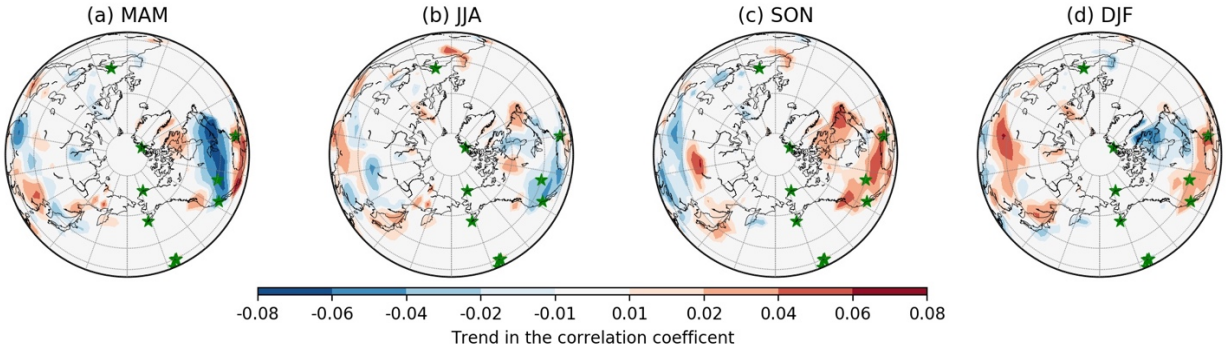

Table S1. Summary of the correlation coefficients between ΔT and ΔSCA from satellite measurements in each continent.

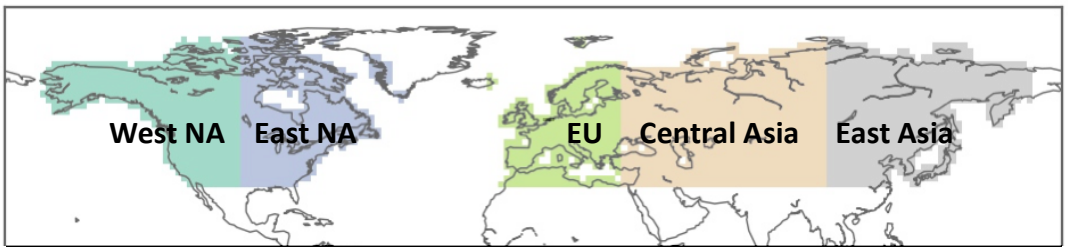

	SCIAMACHY (2003-2011)		GOSAT (2010-2015)	
	r	p	r	p
West NA	-0.22	0.56	**-0.77***	0.07
East NA	-0.26	0.49	-0.33	0.52
West EU	0.41	0.27	-0.07	0.9
West EA	**-0.66***	0.05	-0.22	0.67
East EA	-0.43	0.25	**0.76***	0.08
>30NH	**-0.70***	0.04	-0.52	0.29